BIOCHEMISTRY
including biophysical chemistry & molecular biology

Article

pubs.acs.org/biochemistry

Conformational Analysis and Chemical Reactivity of the Multidomain Sulfurtransferase, *Staphylococcus aureus* CstA

Khadine A. Higgins,[†,#] Hui Peng,[†,‡] Justin L. Luebke,[†] Feng-Ming James Chang,[†] and David P. Giedroc*[,†]

[†]Department of Chemistry, Indiana University, Bloomington, Indiana 47405-7102, United States

[‡]Graduate Program in Biochemistry, Indiana University, Bloomington, Indiana 47405, United States

Supporting Information

ABSTRACT: The *cst* operon of the major human pathogen *Staphylococcus aureus* (*S. aureus*) is under the transcriptional control of CsoR-like sulfurtransferase repressor (CstR). Expression of this operon is induced by hydrogen sulfide, and two components of the *cst* operon, *cstA* and *cstB*, protect *S. aureus* from sulfide toxicity. CstA is a three-domain protein, and each domain harbors a single cysteine that is proposed to function in vectorial persulfide shuttling. We show here that single cysteine substitution mutants of CstA fail to protect *S. aureus* against sulfide toxicity *in vivo*. The N-terminal domain of CstA exhibits thiosulfate sulfurtransferase (TST; rhodanese) activity, and a Cys66 ^{34}S-persulfide is formed as a catalytic intermediate in both the presence and absence of the adjacent TusA-like domain using ^{34}S-SO_3^{2-} as a substrate. Cysteine persulfides can be trapped on both C66 in CstA^{Rhod} and on C66 and C128 in CstA$^{Rhod\text{-}TusA}$ when incubated with thiosulfate, sodium tetrasulfide (Na_2S_4), and *in situ* persulfurated SufS. C66A substitution in CstA$^{Rhod\text{-}TusA}$ abolishes C128 *S*-sulfhydration, consistent with directional persulfide shuttling in CstA. Fully reduced CstA$^{Rhod\text{-}TusA}$ is predominately monomeric, and high resolution tandem mass spectrometry reveals that Cys66 and Cys128 can form a C66−C128 disulfide bond using a number of oxidants, which leads to a significant change in conformation. A competing intermolecular C128−C128′ disulfide bond is also formed. Small-angle X-ray scattering measurements and gel filtration chromatography of reduced CstA$^{Rhod\text{-}TusA}$ reveal an elongated molecule ($R_g \approx 30$ Å, 21.6 kDa) where the two domains pack "side-by-side" that likely places Cys66 and Cys128 far apart. These studies are consistent with the low yield of C66−C128 cross-link as a mimic of a persulfide transfer intermediate in CstA, and small, but measurable persulfide transfer from Cys66 to Cys128 within the CstA$^{Rhod\text{-}TusA}$ with inorganic sulfur donors.

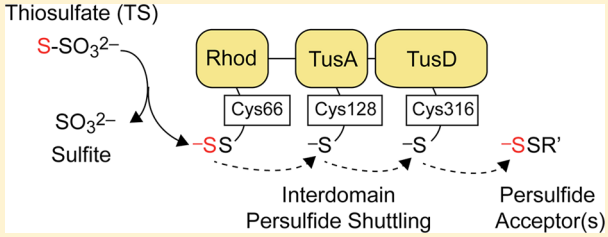

The Gram-positive opportunistic pathogen *Staphylococcus aureus* is the causative agent of minor skin infections and a wide range of hospital and community-acquired infections, with the incidence of methicillin-resistant strains continuing to increase in previously low-prevalence areas.[1] New antibiotic therapies that target novel metabolic pathways are therefore urgently needed. Targeting sulfur metabolism or hydrogen sulfide homeostasis[2] is one such strategy since recent work in *Mycobacterium tuberculosis*[3,4] has identified novel features of sulfate assimilation and cysteine biosynthesis[5] as emerging antimicrobial[6] and vaccine[7] strategies.

We previously described a paralog of a copper-sensing transcriptional repressor CsoR (*c*opper-*s*ensitive *o*peron *r*epressor)[8,9] in *S. aureus* strain Newman that we denoted CstR, for *C*soR-like *s*ulfurtransferase *r*epressor.[10,11] CstR is a persulfide and polysulfide-regulated repressor[12] that regulates the expression of an operon, *cst*, which encodes a putative sulfite/sulfonate effluxer (TauE), sulfide-quinone reductase (SQR) as well as two multidomain proteins denoted CstA and CstB that harbor canonical thiosulfate sulfurtransferase (TST) or rhodanese (Rhod) domains of unknown function.[10,13,14] Rhodaneses traffic "activated sulfur" as cysteine persulfides, R-SSH, which, like cysteine desulfurases,[15] make oxidized sulfur bioavailable for downstream persulfide acceptors. Previous studies[12] show that *cstA* and *cstB* as well as *sqr* are important for the viability of *S. aureus* under H_2S stress. Sulfide is toxic and derives from both endogenous and exogenous sources;[16] as a result, sulfide levels must be regulated in cells via efflux, assimilation or oxidation to innocuous sulfur compounds, e.g., thiosulfate (TS) or sulfate. The *cst* operon encodes genes that are predicted to function in sulfur assimilation (*cstA*) and sulfide oxidation (*sqr*, *cstB*).[12]

Multidomain proteins that harbor rhodanese sulfurtransferase domains (Rhod), or more generally, rhodanese homology domains (RHD), are structurally and mechanistically poorly understood.[13] *S. aureus* CstA harbors three domains shown to function in sequential cysteine persulfide transfer in other systems. These include an N-terminal Rhod domain, a middle domain that is homologous to *Escherichia coli* TusA (20% identity; 40% similar) and harbors an active site Cys within a ^{128}CPEP^{131} sequence,[17] and a C-terminal domain that is homologous to TusD within the TusBCD heterohexamer involved in 2-thiouridine (s^2U) tRNA biosynthesis,[18] and *Allochromatium vinosum* DsrE, which as a DsrEFH hetero-

Received: January 21, 2015
Revised: March 19, 2015
Published: March 20, 2015

DOI: 10.1021/acs.biochem.5b00056
Biochemistry 2015, 54, 2385−2398

hexamer, is involved in sulfur oxidation by phototrophic and chemotrophic sulfur bacteria.[19] Each domain contains one of only three Cys in the molecule (Cys66, Cys128, and Cys316) (Figure 1). It is known that in 2-thiouridine biosynthesis TusA

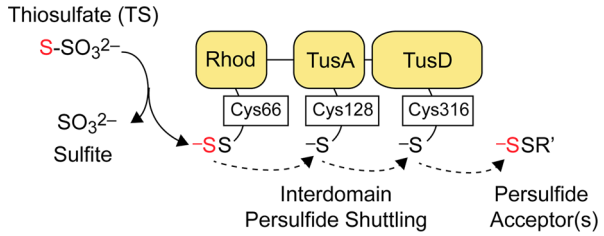

Figure 1. Cartoon representation of vectorial persulfide shuttling in *S. aureus* CstA as a three domain protein harboring an N-terminal rhodanese (Rhod) domain, a central TusA domain, and a C-terminal TusD domain. Each domain contains a single Cys as indicated. A model for persulfide shuttling using TS as a substrate from the N-terminal Rhod is shown. We confirm in this work that a persulfide can be shuttled from Cys66 to Cys128 (*vide infra*), with the Cys128-Cys316 transfer step speculation at present. Other sulfane sulfur sources can substitute for TS, including tetrasulfide and *S*-sulfhydrated SufS (*vide infra*).

acquires its persulfide group directly from the cysteine desulfurase IscS, which then shuttles it to TusD. We therefore propose that the three domains of CstA function to sequentially "shuttle" sulfur along a defined path as cysteine persulfides (Figure 1) via sequential nucleophilic attack of an acceptor thiolate with the terminal sulfur of the donor persulfide. This model predicts that well-defined interdomain interactions in CstA control the specificity and directionality of the relay, while minimizing potential side reactions of persulfide intermediates with low molecular weight (LMW) thiols, which would liberate toxic sulfide by reacting with oxidized thiols *in situ*.[14]

Although rhodaneses and rhodanese homology domains are widespread in nature, their biological functions in large measure remain enigmatic. Rhod domains are found as isolated "single-domain" proteins, the structural prototype of which is *E. coli* PspE,[20] as tandem double[21,22] and triple Rhod domain proteins, one of which is involved in molybdopterin biosynthesis in *E. coli*,[23,24] or as a single Rhod domain within a multidomain protein.[25−27] In the latter case, as is *S. aureus* CstA, the Rhod domain is sometimes fused with other domains projected to play roles in persulfide chemistry and/or sulfur shuttling and sulfur reduction.[13,27] *S. aureus* strain Newman encodes two other single-domain rhodaneses (NWMN_1438, NWMN_1650[2]), one other putative multidomain sulfurtransferase (NWMN_2587), and one other TusA (NWMN_1951) elsewhere in the genome. Although the function of TusA homologues outside of 2-thiouridine biosynthesis in *E. coli* is not well understood, a single-domain TusA-like protein in *Pseudomonas aeruginosa* (PA1006) has been shown to play a role in persulfide chemistry in molybdenum homeostasis[28] associated with molybdenum cofactor (MoCo) biosynthesis and maturation of nitrate reductase, all processes that are important for nitrate respiration, biofilm formation, and virulence in that organism.[29]

Other functional roles for rhodaneses beyond persulfide chemistry are becoming apparent. For example, an *E. coli* strain lacking DsbA leads to overexpression of the periplasmic rhodanese, PspE, which then introduces disulfide bonds in substrate proteins in a process requiring DsbC to make the process catalytic. In the Δ*dsbA* strain, PspE is extensively sulfenylated rather than persulfurated.[30] It is known that persulfurated PspE and other rhodaneses can react with dithiol form of dithiothreitol (DTT) to release sulfide and oxidized dithiothreitol; in addition, rhodaneses also form mixed disulfides with LMW thiols upon reaction with LMW disulfide oxidized thiols,[31] e.g., β-mercaptoethanol as found in the crystal structure of *S. aureus* NWMN_1650.[2] This suggests that the active site Cys in Rhods is versatile and susceptible to a number of modifications, i.e., persulfuration (*S*-sulfhydration), sulfenylation, and mixed disulfide formation (*S*-thiolation). It has also been shown that PspE and GlpE, another single-domain TST from *Salmonella typhimurium*, contribute to virulence in a mouse model of systemic infection, although the mechanisms for this protection are not known.[32]

In this work, we show that single cysteine substitutions of the Rhod, TusA, or TusD domains of CstA fail to protect *S. aureus* strain Newman from hydrogen sulfide toxicity. We establish that the N-terminal Rhod domain of CstA possesses significant thiosulfate sulfurtransferase (TST) activity. Vectorial transfer of the so-formed persulfide intermediate on Cys66 of the Rhod domain in CstA$^{Rhod\text{-}TusA}$ to Cys128 on the downstream TusA domain is observed, particularly when highly reactive sodium tetrasulfide and cysteine desulfurase SufS harboring a cysteine persulfide were used as the source of oxidized sulfur. We demonstrate that the CstA$^{Rhod\text{-}TusA}$ molecule is highly anisotropic, with each domain essentially "side-by-side" with the two Cys in each domain likely far apart. This may serve to limit the extent of interdomain persulfide transfer in the absence of the C-terminal TusD oligomerization domain. However, the Rhod and TusA domain cysteines must come close to one another at least transiently since three separate oxidants catalyze the formation of an intramolecular Cys66-Cys128 disulfide bond. Formation of this disulfide is in competition with the Cys128-Cys128′ cross-linking within what must be a transiently formed CstA$^{Rhod\text{-}TusA}$ oligomer given a dominant monomeric assembly state in solution. The implications of these findings on the function of CstA in *S. aureus* are discussed.

MATERIALS AND METHODS

Plasmid Construction, Protein Expression, and Purification of CstAs. Sections of NWMN_0027, CstA^{Rhod}, and CstA$^{Rhod\text{-}TusA}$, were PCR amplified and subcloned into pET3b and pET15b, respectively. The C66A and C128A CstA$^{Rhod\text{-}TusA}$ mutants were constructed using the following primers, CCTATTATGTAATCGCTAGAAGTGGTAACAGAAG and CTAATTTTTACAATTGGCCCTGGAGCTTGAAG-ACCACGATAG, respectively. All the resultant plasmids were verified by DNA sequencing at the Indiana Molecular Biology Institute (IMBI). Plasmids carrying the wild-type and mutant CstA^{Rhod} and CstA$^{Rhod\text{-}TusA}$ were transformed into separate aliquots of *E. coli* Rosetta (DE3) pLysS competent cells (EMD Millipore). A single colony was grown in a 5 mL culture to an OD of 0.6. The 5 mL culture was used to inoculate a 15 mL culture, which was grown to an OD of 0.6 and used to inoculate a 1 L culture. All cultures were in Luria−Bertani broth supplemented with 100 μg/mL of ampicillin (amp) and grown at 37 °C with shaking. The 1 L culture was grown to an OD_{600} of ∼0.7 and then induced by the addition of isopropyl β-D-1-thiogalatopyranoside (IPTG) to a final concentration of 0.8 mM. Postinduction the cultures were grown at 20 °C with shaking overnight. The cells were centrifuged, resuspended in lysis buffer containing 50 mM HEPES, pH 7.0, 500 mM NaCl 5 mM ethylenediaminetetraacetic acid (EDTA), and 5 mM

DOI: 10.1021/acs.biochem.5b00056
Biochemistry 2015, 54, 2385−2398

dithiothreitol (DTT) and lysed by sonication. After centrifugation, polyethyleneamine (PEI) pH 7.0 was added at a final concentration of 0.15 (v/v) and stirred at 4 °C for 2 h followed by centrifugation.

For $CstA^{Rhod}$, the supernatant was precipitated by the addition of 0.325 g/mL of $(NH_4)_2SO_4$ and stirred 4 °C for 1 h and centrifuged. The supernatant containing $CstA^{Rhod}$ was dialyzed overnight at 4 °C into low salt buffer, 25 mM MES, pH 5.5, 25 mM NaCl, 5 mM DTT, 2 mM EDTA and loaded onto a SP-Sepharose Fast Flow column and fractions eluted in a salt gradient 0.025−0.5 M NaCl. Fractions containing $CstA^{Rhod}$ as determined by an SDS-PAGE gel were pooled, concentrated, and buffer exchanged into 25 mM MES, pH 5.5, 500 mM NaCl, 5 mM DTT, 2 mM EDTA and loaded onto a HiLoad 16/60 Superdex 75 preparative-grade column for final polishing.

For wild-type and mutant $CstA^{Rhod\text{-}TusA}$, the supernatant was precipitated with the addition of 0.15 g/mL and 0.45 g/mL $(NH_4)_2SO_4$ and stirred 4 °C for 1 h and centrifuged. The pellet from the second $(NH_4)_2SO_4$ cut, following resuspension was dialyzed into buffer H, 25 mM HEPES, pH 7.0, 50 mM NaCl, 5 mM DTT, and 2 mM EDTA. The precipitate was removed by centrifugation and the supernatant loaded onto a Q-sepharose column. This column was equilibrated with buffer H and eluted by a linear gradient from 0.050 to 0.5 M NaCl. Fractions containing $CstA^{Rhod\text{-}TusA}$ were concentrated and loaded onto a HiLoad 16/60 Superdex 75 preparative-grade column that was equilibrated with 25 mM HEPES, pH 7.0, 200 mM NaCl, 5 mM DTT, and 2 mM EDTA. Fractions containing $CstA^{Rhod\text{-}TusA}$ were further purified using a MonoQ 5/50 GL column that was also equilibrated with buffer H. The purity of the protein fractions was checked by SDS-PAGE gels, with the identity of proteins verified by liquid chromatography electrospray ionization mass spectrometry (LC-ESI/MS). Protein concentrations were determined using ϵ_{280} of 11 920 M^{-1} cm^{-1} and 21 890 M^{-1} cm^{-1} for $CstA^{Rhod}$ and $CstA^{Rhod\text{-}TusA}$, respectively, as calculated from Protein Prospector.

Plasmid Construction, Protein Expression, and Purification of N-Terminally His-tagged SufS. Various subregions of the gene encoding NWMN_0787 were subcloned into the pHis-parallel plasmid[33] using the primer ATGGTGAATGAAGTGGCCGAACACTCATTT-GACG. All the resultant plasmids were verified by DNA sequencing at the IMBI. The plasmid carrying the wild-type SufS was transformed into *E. coli* Rosetta (DE3) pLysS competent cells (EMD Millipore). A single colony was grown in a 100 mL overnight culture, and 10 mL of this culture was used to inoculate 1 L cultures. All cultures were in Luria−Bertani broth supplemented with 100 μg/mL of amp and grown at 37 °C with shaking. The 1 L culture was grown to an OD_{600} of ∼0.8 and then induced by the addition of IPTG to a final concentration of 0.8 mM. Post induction the cultures were grown at 16 °C with shaking overnight. The cells were pelleted and resuspended in lysis buffer, 25 mM Tris, pH 8.0, 200 mM NaCl, 5 mM Tris(2-carboxyethyl)phosphine hydrochloride (TCEP), 10 mM imidazole and lysed by sonication. After centrifugation, the supernatant was loaded onto a HisTrap FF column (GE Healthcare), and the recombinant protein was eluted in the 25 mM Tris, pH 8.0, 200 mM NaCl, 5 mM TCEP, 250 mM imidazole. The identity of proteins was verified by matrix-assisted laser desorption ionization time-of-flight (MALDI-TOF) mass spectrometry. Protein concentrations were determined by A_{280nm} using an extinction coefficient of 47 790 M^{-1} cm^{-1}.

Preparation of *S. aureus* Strain Newman Complementation Strains and Growth Curves. The construction of the Δ*cstA* (NWMN_0027) strain was described previously.[12] Genes were cloned into the pOS1 vector containing the P_{lgt} constitutive promoter[34] between the *Nde*I and *Bam*HI restriction sites and sequenced using appropriate primers. Each construct was electroporated into *S. aureus* RN4220 to obtain a properly methylated plasmid prior to electroporation into *S. aureus* strain Newman. Wild-type (WT) *S. aureus* was complemented with empty vector. Plasmid DNA was maintained by addition of 10 μg/mL chloramphenicol to the plates and liquid growth media.

Fresh TSB broth (5 mL broth, 50 mL Falcon tubes) was inoculated with *S. aureus* strains from frozen glycerol cell stocks and grown to stationary phase overnight with shaking (∼14 h, 37 °C, 200 rpm). A 1 mL aliquot was pelleted by centrifugation and resuspended in an equal volume Hussain−Hastings−White modified (HHWm) minimal media[10,35,36] and then diluted in 15 mL TSB or HHWm supplemented with 0.5 mM thiosulfate as described in previous work.[12] For samples grown in the presence of NaHS, 0.2 mM was added at t = 0. The starting OD_{600} of each culture was approximately 0.007, and cell density was measured hourly for 10 h. All cultures were grown in the presence of 10 μg/mL chloramphenicol unless otherwise noted.

Thiosulfate and 3-Mercaptopyruvate Sulfurtransferase Activity Assays. Thiosulfate sulfurtransferase (rhodanese) activity was determined for $CstA^{Rhod}$ as well as wild-type C66A and C128A $CstA^{Rhod\text{-}TusA}$, monitoring the formation of Fe(III) thiocyanate.[37,38] Briefly, a 1 mL reaction mixture containing 50 mM KCN, 100 mM MES, pH 6.0 for $CstA^{Rhod}$ or 100 mM HEPES, pH 7.0 for $CstA^{Rhod\text{-}TusA}$ and thiosulfate (100−4000 μM) was first clarified by centrifugation at 3000 rpm for 2 min and the supernatant was incubated at 37 °C for 4 min. The reaction was initiated by the addition of the enzyme (0.4 μM) and incubated at 37 °C for an additional 4 min. The reaction was stopped by addition of 2 mL of the iron reagent (0.5 mL formaldehyde mixed with 1.5 mL 123 mM ferric nitrate nonahydrate dissolved in 13% HNO_3). The reaction was centrifuged at 3000 rpm for 5 min and 350 μL was pipetted into 96 well plates and $FeSCN^{2+}$ detected at 460 nm using a Bioteck Synergy H1 hybrid Multimode microplate reader. Standard curves were obtained by incubating a known concentration of potassium thiocyanate (KSCN) with the iron reagent and measuring absorbance of 460 nm.[38] The same experiment was repeated for $CstA^{Rhod}$ using 3-mercaptopyruvate (3-MP) as a substrate, with 1 mL reactions containing 50 mM KCN, 5 mM 3-MP, and 0.42 μM enzyme as described.[37]

Reactions with ^{34}S and ^{32}S Thiosulfate (TS). All CstA-derived proteins were treated with a 20-fold molar excess of KCN in 100 mM Tris pH 8.0 and incubated at room temperature for 1 h to remove any cysteine persulfide present following purification.[39] For the reactions with ^{34}S and ^{32}S thiosulfate, proteins were buffer-exchanged under anaerobic conditions into 10 mM HEPES, pH 7.0 and 200 mM NaCl and incubated with a 25-fold excess of ^{34}S TS and ^{32}S TS for 1 h. The reactions were quenched by addition of 8 M urea, 100 mM iodoacetamide in 50 mM Tris pH 8.0 with incubation in the dark for 30 min, precipitated with a 25% final concentration of trichloroacetic acid (TCA) and placed on ice for 1 h. The solution was centrifuged, and the pellets were washed twice with cold acetone, centrifuged, dried, and resuspended in 20 μL of 15 mM ammonium bicarbonate pH 8.0 with 10% acetonitrile. Proteomics grade trypsin was added at a 1:50 ratio and the protein was digested at 37 °C for 1 h. A final concentration of 0.25−1.0% trifluoroacetic acid (TFA) was added to quench the

DOI: 10.1021/acs.biochem.5b00056
Biochemistry 2015, 54, 2385−2398

digest followed by spotting on a MALDI plate with α-cyanocinnamic acid (CCA) matrix with a 5:1 matrix/sample ratio for analysis. MALDI-TOF mass spectra were collected and analyzed using a Bruker Autoflex III MALDI-TOF mass spectrometer with 200 Hz frequency-tripled Nd:YAG laser (355 nm) and Flex Analysis software (Bruker Daltonics, Billerica, MA). Cysteine-containing peaks were identified by monoisotopic mass (Tables S1−S3, Supporting Information). The theoretical distribution and peak areas were determined using the averagine algorithm[40] and quantified by summing the total peak areas of the full isotopic distribution. Iodoacetamide alkylation efficiencies of the thiol and persulfide over all experiments (TS, NaHS*, Na_2S_4, and SufS-SSH) using this protocol were 92 (±15% s.d.) and 91 (±17%), respectively, with no statistically significant differences between alkylation of C66 versus C128.

Reactions with NaHS and Na_2S_4. Reactions with NaHS and Na_2S_4 were performed in 25 mM Tris, pH 8.0, 200 mM NaCl under anaerobic conditions. 100 μL aliquots of 25 μM CstA protein were incubated with a 20-fold sulfur excess of NaHS, and Na_2S_4 the reactions were incubated for 5 min and quenched with an equal volume of 8 M urea, 200 mM iodoacetamide in 50 mM Tris, pH 8.0. Samples were TCA-precipitated and digested with trypsin and peptides were analyzed by MALDI-TOF MS and quantified as described above. The NaHS used in these experiments is known to be contaminated with detectable polysulfide impurities[12] and thus exhibits a reactivity profile that is similar to that of Na_2S_4; these reactions are denoted NaHS* (Table S2, Supporting Information).

Reactions with *S. aureus* SufS, Pyridoxal 5′-Phosphate (PLP) and Cysteine. $CstA^{Rhod}$, wild-type, and C66A $CstA^{Rhod\text{-}TusA}$ were incubated with an equimolar concentration of fully reduced SufS, a 5-fold molar excess of PLP, and a 25-fold excess cysteine. A control reaction was performed for each CstA derivative where SufS protein was left out. Reactions were allowed to incubate for 10, 20, 30, 60, and 120 min as well as overnight. All reactions were performed in 25 mM Tris, pH 8.0, 200 mM NaCl under anaerobic conditions. The reactions mixtures were quenched with an equal volume of 8 M urea, 200 mM iodoacetamide in 50 mM Tris pH 8.0, TCA-precipitated, and digested with trypsin, and peptides were analyzed by MALDI-TOF MS and quantified as described above.

$CstA^{Rhod\text{-}TusA}$ Oxidation, Size Exclusion Chromatography, and Tandem Mass Spectrometry. Samples of ∼50 μM $CstA^{Rhod\text{-}TusA}$, C66A $CstA^{Rhod\text{-}TusA}$, and C128A $CstA^{Rhod\text{-}TusA}$ were removed from a Vacuum Atmospheres (Amesbury, MA) glovebox under an inert argon atmosphere and allowed to oxidize on the benchtop for 24 or 48 h in Buffer A (10 mM HEPES, 200 mM NaCl, pH 7.0). Oxidized (24 h) $CstA^{Rhod\text{-}TusA}$ was TCA precipitated and resuspended in 10 mM ammonium acetate at pH 8.0 and digested with trypsin at 37 °C for 1 h, as described above. A final concentration of ∼1% TFA was added to quench the digest and acidify the sample prior to tandem mass spectrometry.

A 100 μL sample of ∼50 μM $CstA^{Rhod\text{-}TusA}$ was injected onto an analytical G-75 Superdex 10/300 gel filtration column (GE Healthcare) on an Akta FPLC system (GE Healthcare) at a flow rate of 0.75 mL/min. The column and FPLC were equilibrated with Buffer A. For the reduced sample, 5 mM DTT was added to Buffer A to ensure $CstA^{Rhod\text{-}TusA}$ cysteines remained reduced. The estimated molecular weight was determined using a calibration curve obtained with globular protein standards (GE Healthcare). Tandem mass spectrometry of $CstA^{Rhod\text{-}TusA}$ peptides was performed using a ThermoFinnigan LTQ-Orbitrap XL mass spectrometer (San Jose, CA) equipped with an UltiMate 3000 nanoLC system (Dionex, Sunnyvale, CA) at the Laboratory for Biological Mass Spectrometry essentially as described.[11,41] Briefly, 5 μL of tryptically digested protein was loaded onto a 15 mm × 100 mm i.d. C18 reversed-phase trapping column and eluted through a 150 mm × 75 mm internal diameter analytical

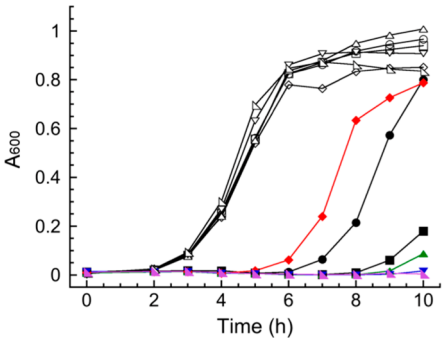

Figure 2. Growth curves of wild-type and Δ*cstA* mutant *S. aureus* strains transformed with the indicated CstA allele carried on the pOS1 complementation vector.[12] Cultures were grown under aerobic conditions in HHWm + TS minimal media at 37 °C with shaking in the absence (open symbols; all black) and presence (filled symbols, differently shaded) of 0.2 mM NaHS added to the growth medium at t = 0. Wild-type (circles, black), Δ*cstA* (squares, black), Δ*cstA*:CstA (diamonds, *red*); Δ*cstA*:$CstA^{C66A}$ (triangles, green); Δ*cstA*:$CstA^{C128A}$ (upside down triangles, blue); Δ*cstA*:$CstA^{C316A}$ (right-facing triangles; purple).

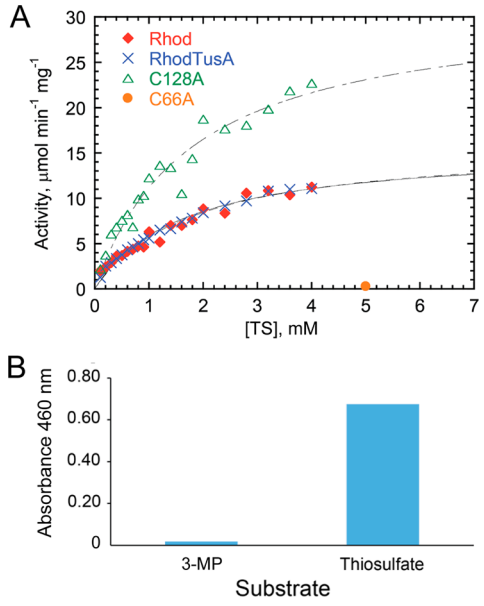

Figure 3. N-terminal Rhod domain of CstA possesses thiosulfate (TS) sulfurtransferase activity but no 3-mercaptopyruvate (3-MP) sulfurtransferase activity. (A) Kinetic analysis of $CstA^{Rhod}$ and $CstA^{Rhod\text{-}TusA}$ using thiosulfate (TS) as a substrate. Enzyme activity was measured as a function of [TS] using a standard colorimetric rhodanese activity assay that employs KCN as the reductant[31] (see Materials and Methods) with the continuous line a nonlinear least-squares fit to a simple Michaelis−Menten model which returns the following parameters: $CstA^{Rhod}$: K_m = 1.8 ± 0.3 mM; V_{max} = 16 ± 1 μmol min^{-1} mg^{-1} protein;: $CstA^{Rhod\text{-}TusA}$: K_m = 1.7 ± 0.1 mM; V_{max} = 15.6 ± 0.6 μmol min^{-1} mg^{-1} protein; C128A $CstA^{Rhod\text{-}TusA}$, K_m = 1.8 ± 0.3 mM; V_{max} = 31 ± 3 μmol min^{-1} mg^{-1} protein. No turnover is observed with C66A $CstA^{Rhod\text{-}TusA}$. (B) Single time-point analysis of $CstA^{Rhod}$ and $CstA^{Rhod\text{-}TusA}$ using 3-mercaptopyruvate (3-MP) as a substrate.

DOI: 10.1021/acs.biochem.5b00056
Biochemistry 2015, 54, 2385−2398

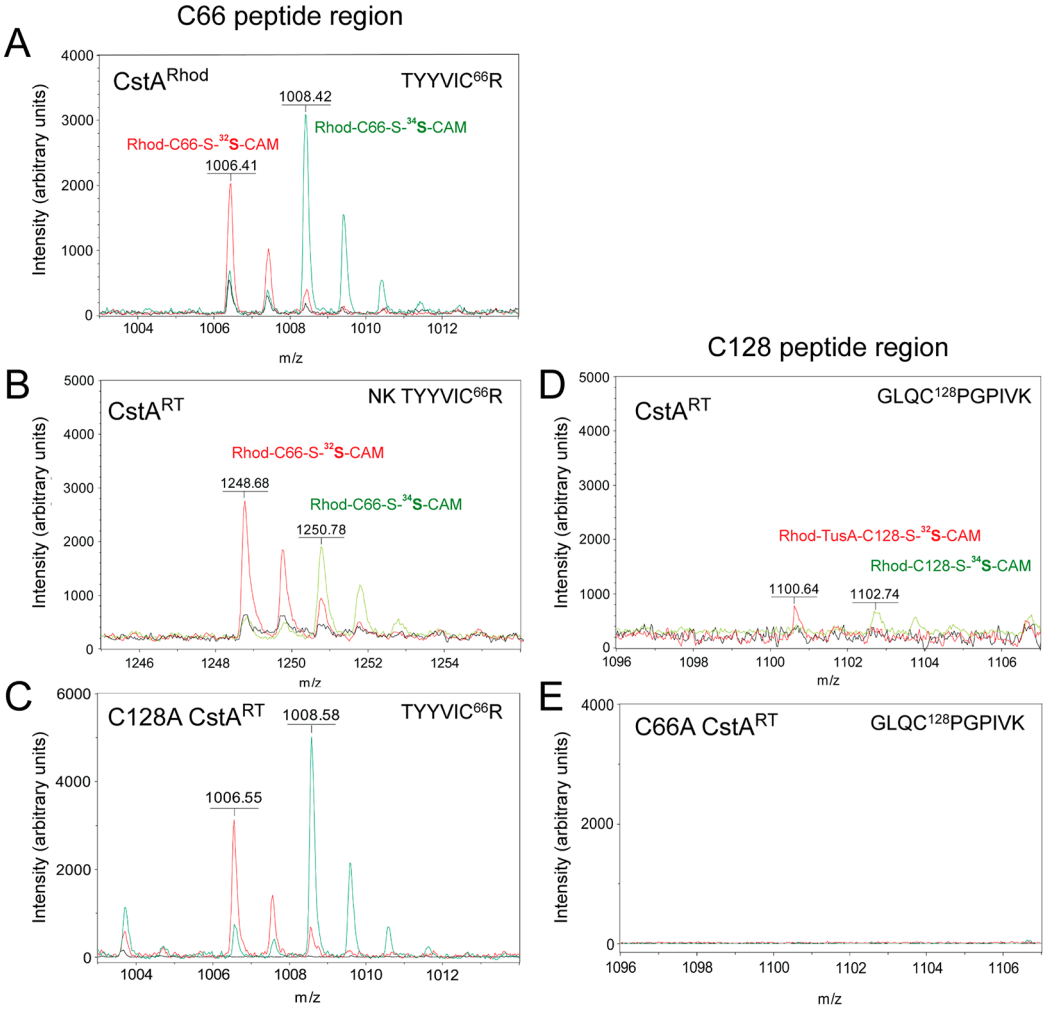

Figure 4. Analysis of cysteine *S*-sulfhydration products of (A) $CstA^{Rhod}$, (B, D) $CstA^{Rhod\text{-}TusA}$ (denoted $CstA^{RT}$) and (C) C128A $CstA^{Rhod\text{-}TusA}$ and (E) C66A $CstA^{Rhod\text{-}TusA}$ incubated with $^{32}S{-}^{32}SO_3$ (red trace) or $^{34}S{-}^{32}SO_3$ (green trace) compared to the corresponding unreacted starting material (black trace) by MALDI-TOF mass spectrometry following tryptic digestion (see Materials and Methods). The mass spectral region of highest intensity is shown for each peptide (sequence shown, upper right) indicative of *S*-sulfhydration of Cys66 (left panels) or C128 (right panels). The nature of the adducts formed in each case is indicated. The yield of C128 persulfide is 3.3% (panel D) and 0% (panel E). See Table S1 for an accounting of all peptides observed. Conditions: 25 μM protein incubated with 25-fold excess of $Na_2S_2O_3$ for 1 h, 25 mM Tris-HCl, pH 8.0, 200 mM NaCl, ambient temperature, anaerobic conditions.

column packed with 5 μm, 100 Å Magic C18AQ packing material (Microm BioResourses Inc., Auburn, CA), using a 30 min gradient from 97% to 60% solvent A, 97:3:0.1 water/acetonitrile/formic acid (solvent B is 0.1% formic acid in acetonitrile) at 250 nL/min. Eluting peptides were ionized and electrosprayed directly and "top-five" data-dependent tandem mass spectra were recorded. Cross-linked peptides were identified manually by monoisotopic mass and confirmed by investigation of the fragmentation pattern. For MALDI-TOF mass spectrometry, the digested proteins were mixed with the CCA matrix at a 5:1 ratio, 1 μL was spotted on a MALDI plate. Data were collected on a Bruker Biflex III MALDI TOF instrument and analyzed and quantified as described above.

Small Angle X-ray Scattering (SAXS) Data Collection and Analysis. All SAXS data were acquired at Sector 12ID-B of the Advanced Photon Source at the Argonne National Laboratory. The energy of the X-ray beam was 12 keV (λ = 1.033 Å), with the acquisition parameters adjusted to achieve scattering q values of $0.005 < q < 0.993$ Å^{-1}, where $q = (4\pi/\lambda)\sin\theta$, and 2θ is the scattering angle. All samples were prepared at three different concentrations (1, 3, 5 mg/mL) with an exact buffer match. The buffer was 25 mM HEPES, pH 7.0, 200 mM NaCl, 2 mM TCEP, 5 mM EDTA. Twenty two-dimensional images were recorded for each buffer or protein sample using a flow cell, with an exposure time of 0.5 s to minimize radiation damage and obtain a acceptable signal-to-noise. The 2D images were reduced to one-dimensional scattering profiles using Matlab software on-site. Corrected scattering curves were obtained by subtracting buffer scattering from sample scattering using PRIMUS.[42] Zero concentration extrapolations from three concentration curves were performed in PRIMUS to remove attractive or repulsive interactions factors. Estimates of the radius of gyration (R_g) were obtained using the Guinier approximation $\ln(I(q)) \approx \ln(I(0)) - R_g^2q^2/3)$ from data at low q values in the range of $qR_g < 1.3$. Data points were used with q up to $8/R_g$ to generate a real space pair distance distribution function (PDDF or P(r)) using GNOM,[43] with D_{max} calibrated until the PDDF curve fell smoothly to zero. *Ab initio* modeling was performed using the program DAMMIF[44] to obtain 15 dummy bead models. These models were averaged in

DOI: 10.1021/acs.biochem.5b00056
Biochemistry 2015, 54, 2385−2398

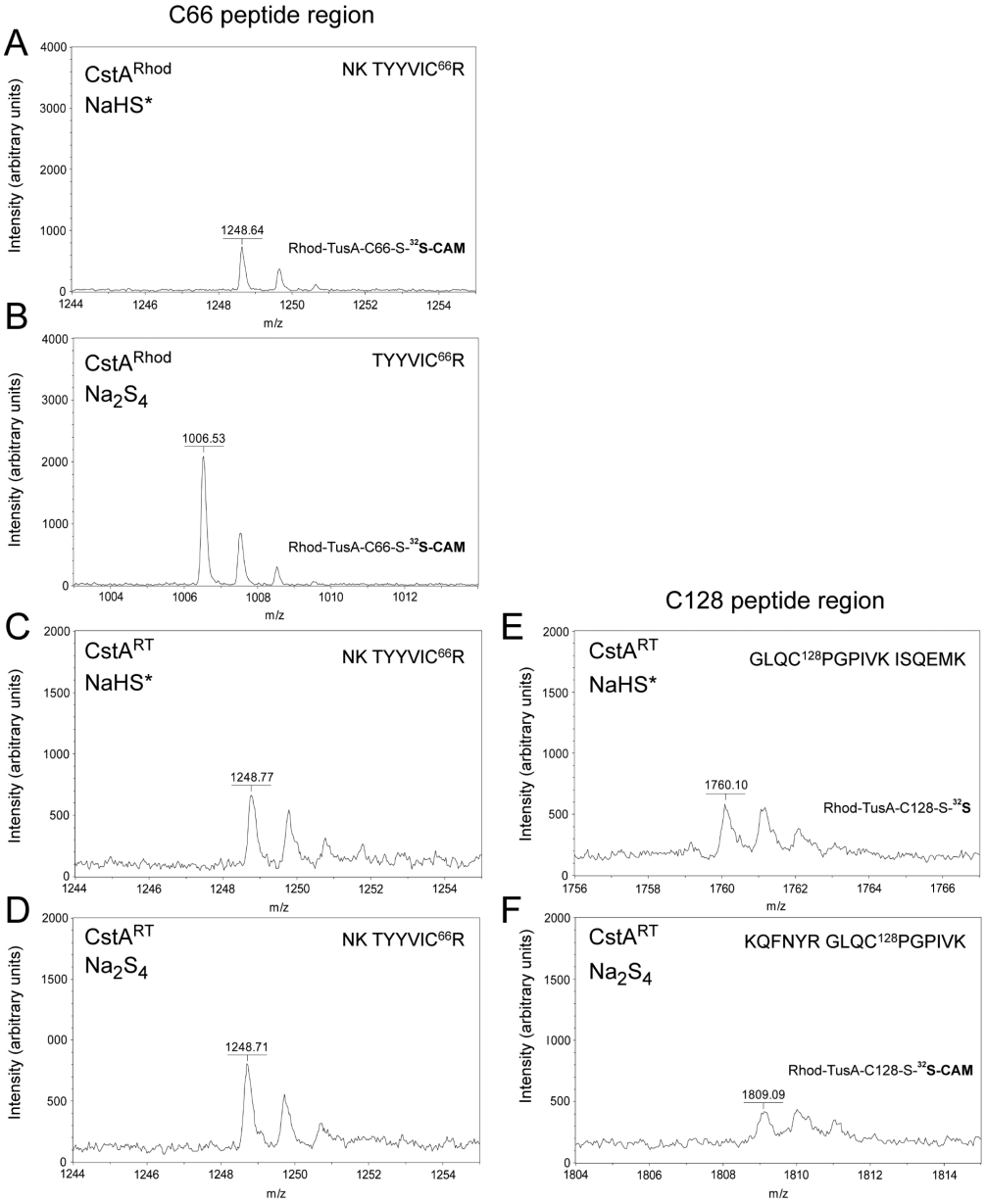

Figure 5. Analysis of cysteine *S*-sulfhydration products of (A, B) $CstA^{Rhod}$ and (C–F) $CstA^{Rhod\text{-}TusA}$ ($CstA^{RT}$) incubated with either NaSH* (panels A, C, and E) or sodium tetrasulfide (panels B, D, and F) as analyzed by MALDI-TOF mass spectrometry following tryptic digestion (see Materials and Methods). The mass spectral region of highest intensity is shown for each peptide (sequence shown, upper right) indicative of *S*-sulfhydration of Cys66 (left panels) or C128 (right panels). Note that panels C and E and D and F are derived from the same tryptic digests. The yield of C128 persulfide is 24% (panel E) and 68% (panel F). See Table S2 for an accounting of all peptides observed. Conditions: 25 μM protein incubated with 25-fold sulfur excess for 5 min, 25 mM Tris-HCl, pH 8.0, 200 mM NaCl, ambient temperature, anaerobic conditions.

DAMAVER[42] with normalized spatial discrepancy (NSD) less than 1.0, indicating good agreement between individual models. Smooth envelopes were superimposed on the crystal structures of an *S. aureus* single-domain rhodanese (NWMN_1650; pdb 3IWH[a]) and TusA extracted from the coordinates of the *E. coli* IscS-TusA complex (pdb 3LVJ[17]) using SUPCOMB.[45] The theoretical scattering intensity of the atomic model of *S. aureus* Rhod (NWMN_1650; pdb 3IWH[a]) was calculated and fitted to the experimental scattering intensity using the FoXS server.[46,47]

RESULTS

CstA Is Required for Cellular Resistance against Hydrogen Sulfide. Previous studies established that CstR-regulated genes, including *cstA*, are required to protect *S. aureus* Newman strain from hydrogen sulfide toxicity relative to an isogenic wild-type strain grown on a chemically defined HHWm growth medium with 0.5 mM thiosulfate as sole sulfur source (HHWm + TS), and 0.2 mM NaHS added to the growth medium at t = 0.[12] This experiment is recapitulated here to allow a direct comparison of complementation of the Δ*cstA* strain with wild-type vs single-cysteine substitution mutants of CstA (Figure 2).

As reported previously, addition of 0.2 mM NaHS to wild-type cultures gives rise to a significant growth delay, but the cells eventually recover and grow with growth rates similar to unstressed cells. The Δ*cstA* strain, on the other hand, is characterized by a far longer lag phase and only begins to recover at 9 h, suggesting that *cstA* is required to mitigate the effects of

DOI: 10.1021/acs.biochem.5b00056
Biochemistry 2015, 54, 2385–2398

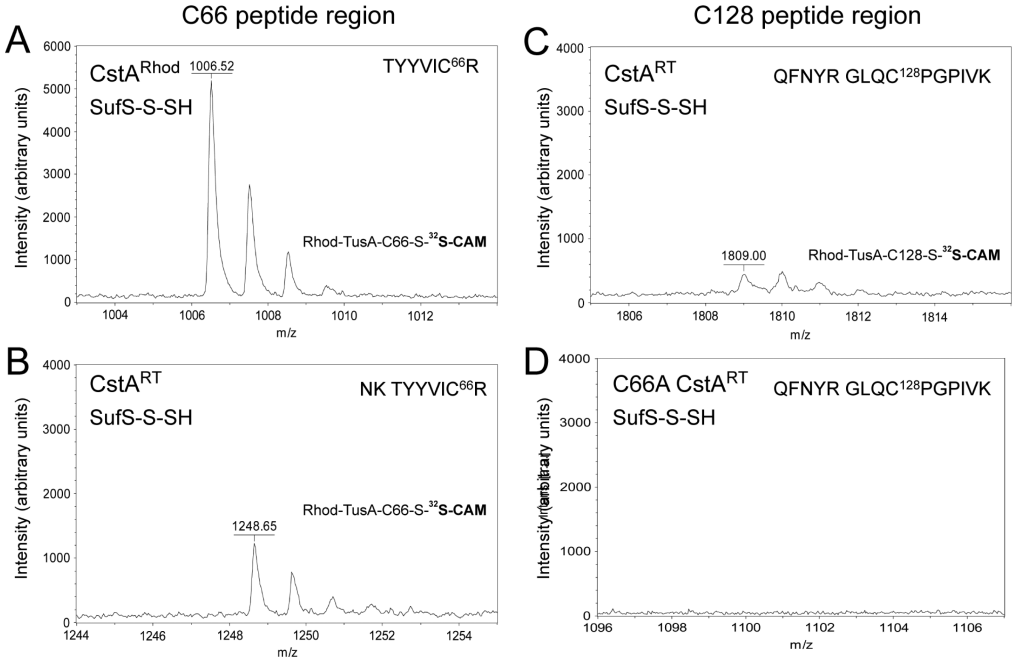

Figure 6. Persulfide transfer from *in situ*-generated SufS persulfide (SufS-S-SH) to CstA. The indicated CstA (CstA^{Rhod} or CstA$^{Rhod\text{-}TusA}$; RT, Rhod-TusA) was incubated with equimolar SufS, and excess PLP and cysteine for either 2 h (panels A–C) or overnight (panel D), alkylated with iodoacetamide, digested with trypsin, and analyzed by MALDI-TOF mass spectrometry (see Materials and Methods). The mass spectral region of highest intensity is shown for each peptide (sequence given) indicative of *S*-sulfhydration of Cys66 (left panels) or C128 (right panels). Note that panels B and C are derived from the same tryptic digest. The yield of C128 persulfide is 100% (panel C) and 0% (panel D). See Table S3 for an accounting of all peptides observed. Conditions: 25 mM Tris-HCl, pH 8.0, 0.2 M NaCl, ambient temperature, anaerobic conditions.

sulfide toxicity. This phenotype is effectively complemented in the Δ*cstA*:CstA strain which directs constitutive expression of *cstA* from the P_{lgt} promoter. This is in strong contrast to Δ*cstA* complementation with individual cysteine mutants of CstA, e.g., Δ*cstA*:CstA^{C66A}, Δ*cstA*:CstA^{C128A}, and Δ*cstA*:CstA^{C316A}, which all fail to restore WT-like growth under hydrogen sulfide stress. These experiments suggest a key functional role played by each cysteine in each domain of CstA in mitigating the effects of cellular sulfide toxicity.

CstA Possesses Thiosulfate Sulfurtransferase Activity. In order to probe the role of individual cysteine residues in CstA, we purified CstA^{Rhod} (residues 1–97) and the two domain molecule, CstA$^{Rhod\text{-}TusA}$ (residues 1–187) to homogeneity under conditions in which both proteins are fully reduced. Cys66 is the presumptive active site Cys in the N-terminal Rhod domain, while Cys128 is the single Cys in the TusA domain (Figure 1). Rhodaneses are known to attack the terminal sulfane sulfur of thiosulfate (TS) to generate an enzyme-bound persulfide and sulfite (Figure 1). The enzyme turns over in the presence of a second reductant which attacks the persulfide sulfur to regenerate the active site cysteine. Cyanide (CN^-) is a convenient exogenous small molecule nucleophile which forms thiocyanate (SCN^-) following reaction with a persulfide. Complexation of SCN^- with Fe(III) results in the formation of a colored ferric thiocyanate complex (λ_{max} = 460 nm). In the persulfide shuttling model (see Figure 1), Cys128 can potentially function as the second nucleophile.

To establish thiosulfate sulfurtransferase (TST) activity of CstA^{Rhod} and CstR$^{Rhod\text{-}TusA}$, each protein was kinetically analyzed using a cyanolysis assay.[31] Figure 3A shows the thiosulfate (TS) concentration-dependence of the formation of the SCN^- with 0.4 μM CstA^{Rhod} or wild-type, C66A or C128A CstA$^{Rhod\text{-}TusA}$. The apparent K_m values determined for Rhod constructs are identical within experimental error at 1.8 mM, revealing the C-terminal TusA domain has no influence on the binding of substrate TS. The V_{max} values determined at 50 mM CN^- differ by a factor of less than two, in the 16-31 μmol min^{-1} mg^{-1} range. The C-terminal TusA domain has only a small stimulatory effect on the turnover of the enzyme, but only when the candidate TusA acceptor is nonfunctional (C128A). The C66A enzyme, in contrast, is inactive revealing that the TST catalytic activity is contained wholly within the Rhod domain. While the K_m for TS is well within the low mM range of other single- and double-domain TSTs, (but not all[48]) the V_{max} is ∼30-fold slower relative to *bona fide* single and double domain TSTs,[13,31] but 150-fold faster than *E. coli* ThiI.[25] CstA^{Rhod} is specific for TS as a sulfur donor, since 3-mercaptopyruvate (3-MP) is not a substrate for this enzyme (Figure 3B). Indeed, *S. aureus*, like many Gram-positive human pathogens, e.g., *Streptococcus*, *Enterococcus*, and *Bacillus*, but unlike *E. coli*, lacks 3-MP sulfurtransferase (3-MST) altogether.[2]

Direct evidence of a CstA-bound persulfide on C66 is shown in Figure 4A. Here, 25 μM reduced CstA^{Rhod} was mixed with 25 mol equiv of either "light" TS, ^{32}S–$^{32}SO_3^{2-}$ or "heavy" TS, ^{34}S–$^{32}SO_3^{2-}$ for 1 h, alkylated with iodoacetamide, subjected to tryptic digestion, and the products were analyzed by MALDI-TOF mass spectrometry Both ^{32}S- and ^{34}S-persulfide containing, carboxyamidomethylated tryptic peptides harboring Cys66, ^{61}TYYVI**C**R or NKTYYVI**C**R (containing a single missed cleavage) are observed using this method for CstA^{Rhod} (Figure 4A), CstA$^{Rhod\text{-}TusA}$ (Figure 4B) and C128A CstA$^{Rhod\text{-}TusA}$ (Figure 4C) (see Table S1 for a complete accounting all peptides detected in this analysis). This experiment provides unambiguous evidence of a persulfide intermediate in the CstA^{Rhod}-catalyzed TST reaction. When this experiment is carried out with wild-type

DOI: 10.1021/acs.biochem.5b00056
Biochemistry 2015, 54, 2385–2398

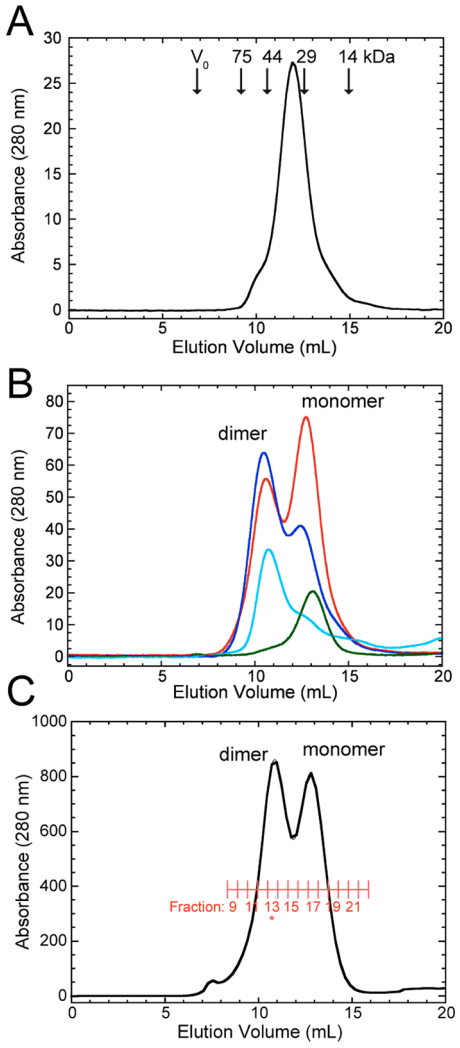

Figure 7. Analytical size exclusion chromatography of (A) fully reduced CstA$^{Rhod\text{-}TusA}$ (50 μM), (B) air-oxidized forms of wild-type and mutant CstA$^{Rhod\text{-}TusA}$ (50 μM), and (C) tetrathionate-oxidized CstA$^{Rhod\text{-}TusA}$. The fractions run on the SDS-PAGE gel shown in Figure 8A are indicated in red. The G75 10/300 elution profile CstA$^{Rhod\text{-}TusA}$ reveals an elution volume of 11.9 mL which corresponds to a molecular weight of 31.5 kDa (21.6 kDa expected) for a spherical protein. In panel (B), the red and blue traces corresponds to 24 and 48 h air oxidation or wild-type CstA$^{Rhod\text{-}TusA}$; cyan trace, 24 h air oxidation of C66A CstA$^{Rhod\text{-}TusA}$; green trace, 24 h air oxidation of C128A CstA$^{Rhod\text{-}TusA}$. Conditions: 10 or 25 mM HEPES, 200 mM NaCl, pH 7.0 using thoroughly degassed buffers. Included volume, V_c = 24.0 mL.

CstA$^{Rhod\text{-}TusA}$, we obtained evidence of persulfide transfer to Cys128 within this two-domain molecule (Figure 4D), although the yield of C128 persulfide was just 3.3% of all recovered C128-containing peptides (Table S1). An initial investigation of the kinetics reveals that under these conditions, below the TS K_m (Figure 3), C66 persulfide accounts for the ≤20% of the total recovered C66-containing peptides (Figure S1; Table S1). However, there is no detectable C128-persulfide obtained when the reaction is carried out with C66A CstA$^{Rhod\text{-}TusA}$ (Figure 4E), consistent with a vectorial relay process in the two domain molecule (Figure 1). Thus, despite the low peptide yields using MALDI further complicated by a number of missed cleavages in peptides harboring Cys128, ^{125}GLQCPGPIVK (*vide infra*), *S*-sulfhydrated and alkylated C128 could be detected in these mixtures (Tables S1−S3).

Table 1. SAXS Structural Parameters Obtained for CstA$^{Rhod\text{-}TusA}$ and CstA^{Rhod}

	CstA$^{Rhod\text{-}TusA}$	CstA^{Rhod}
R_g (Å)[a]	28.2 ± 0.7	19.0 ± 0.4
R_g (Å)[b]	31.1 ± 0.8	16.3 ± 0.1
D_{max} (Å)	116 ± 2	50 ± 2
V_c	269.7	142
$Q_R = V_c^2/R_g$	2580.3	1056.6
MW (kDa)[c]	21.0 (21.6)	8.6 (11.1)
MW (kDa)[d]	25.0 (21.6)	6.6 (11.1)
NSD[e]	0.596 ± 0.022	0.678 ± 0.027
Chi[f]	0.191	0.642

[a]Derived from Guinier fitting (see Figure 10A, insets). [b]Derived from GNOM[43] analysis. [c]Molecular weight calculated from SAXS (using Q_R/0.1231, theoretical molecular weights calculated from protein sequence are shown in parentheses). [d]Molecular weight calculated from excluded volume (bead models). [e]Averaged normalized spatial discrepancy (NSD) from 15 dummy bead models calculated using data points up to $q = 8/R_g$ (see *blue* continuous curves, Figure 10A). [f]Global goodness-of-fit of the theoretical model to the measured scattering data.

Reactivity of CstAs with NaHS* and Sodium Tetrasulfide As Sulfur Donors. Since NaHS and Na_2S_4 added to *S. aureus* strain Newman are potent inducers of the *cst* operon,[12] and the CstA cysteine residues are important for *S. aureus* protection against sulfide toxicity (Figure 2), we tested the ability of CstA^{Rhod} and CstA$^{Rhod\text{-}TusA}$ to react directly with these compounds. Previous studies by a number of groups reveal that commercial sources of NaHS are contaminated by polysulfide impurities, and thus any reaction observed with NaHS is likely attributed to this more oxidized form of sulfur, not S^{2-} itself.[49,50] As a result, reaction profiles obtained with NaHS (denoted NaHS*) and Na_2S_4, with protein thiolates, e.g., in CstR, appear similar.[12] This is the case for CstAs as well (Figure 5; Table S2). Significant persulfide can be trapped and alkylated on C66 in both CstA^{Rhod} (Figure 5A,B) and CstA$^{Rhod\text{-}TusA}$ (Figure 5C,D) in a 5 min reaction with both reagents, with significant persulfide also found on C128 (Figure 5E,F; Table S2). Since C66A CstA$^{Rhod\text{-}TusA}$ gives no reaction products at C128 (Table S2), this result, as with TS above, is consistent with directional relay of the persulfide from C66 to C128.

Reactivity of CstA with a Macromolecular Organic Persulfide As a Sulfur Donor. Previous studies establish that the cysteine desulfurase IscS, involved in Fe−S cluster assembly, forms a diverse range of functional protein−protein complexes with the scaffolding protein IcsU, authentic TusA, and the rhodanese RhdA, each of which mediate sulfur transfer from IscS to these acceptor proteins.[17] *S. aureus* Newman appears to encode two PLP-dependent type I cysteine desulfurases, denoted SufS (NWMN_0787) and NifS (NWMN_1610), the latter of which is projected to be involved in thiamin and/or 4-thiouridine biosynthesis, given its genomic proximity to *thiI*. We therefore tested the ability of the cysteine desulfurase SufS to donate a persulfide to CstA, with the cysteine persulfide on SufS generated *in situ* upon addition of pyridoxal-5′-phosphate (PLP) and cysteine to reactions containing SufS and CstA. These incubations result in significant cysteine persulfide formation on C66 in both CstA^{Rhod} (Figure 6A) and CstA$^{Rhod\text{-}TusA}$ (Figure 6B), with significant C128 persulfide detected in the CstA$^{Rhod\text{-}TusA}$ reaction (Figure 6C, Table S3), which is again abolished in the C66A CstA$^{Rhod\text{-}TusA}$ mutant (Figure 6D). Omission of SufS from these reactions also abolishes product formation

DOI: 10.1021/acs.biochem.5b00056
Biochemistry 2015, 54, 2385−2398

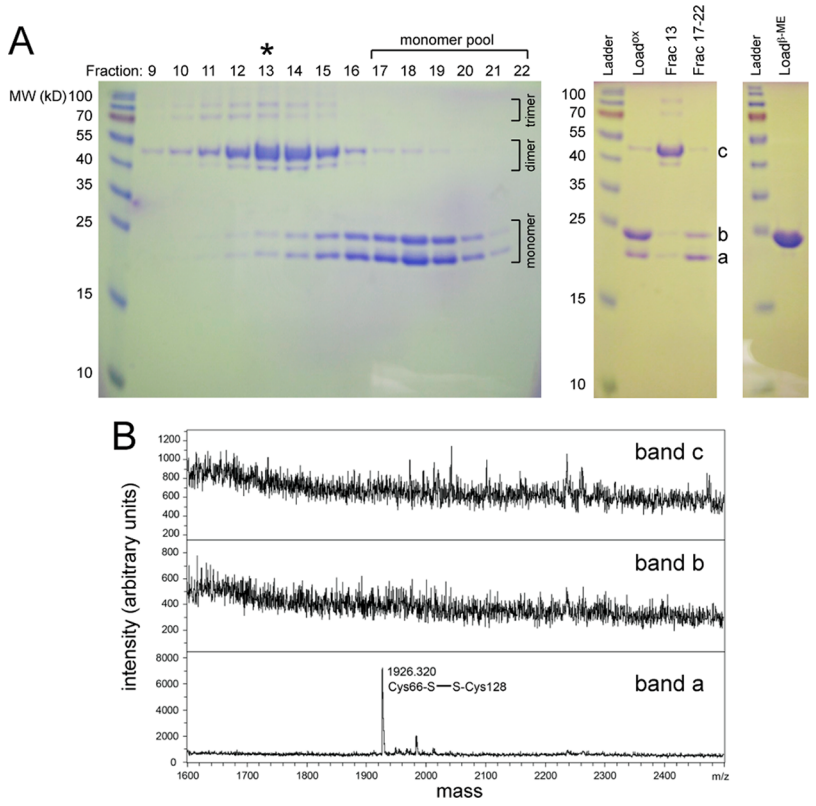

Figure 8. SDS-PAGE analysis of fractions resolved by gel filtration chromatography of the 17 h tetrathionate-induced oxidation of fully reduced CstA$^{Rhod\text{-}TusA}$ shown in Figure 3C. Left panel, fractions 9−22 run on a denaturing, nonreducing gel. Center panel, MW ladder; load (post tetrathionate oxidation); dimer fraction 13; pooled monomer fraction (17−22). The bands labeled a, b, and c were subjected to in-gel tryptic digestion with resulting MS spectra shown in panel (B). Right panel, MW ladder, load (post-tetrathionate oxidation) run on a reducing (β-mercaptoethanol) SDS-PAGE gel. (B) Subsection of the MALDI-TOF spectra focusing on the region expected to contain a peptide corresponding to the C66−C128 cross-link in gel bands a, b, and c from panel (A). This cross-linked peptide is only found in gel band a.

(Figure S2). Overall yields of the persulfide on C66 approach 100% (Figure S3A), with more persulfide on C128 observed vs C66 at early time points (Figure S3B) suggesting that SufS stimulates intramolecular persulfide transfer between C66 and C128. These findings reveal that SufS can function as a persulfide donor to CstA, and the obligatory entry point appears to be C66 in the Rhod domain rather then C128 in the TusA domain.

Disulfide Cross-Linking as a Probe of CstA$^{Rhod\text{-}TusA}$ Conformation. The experiments described above provide evidence of persulfide shuttling between the Rhod and TusA domain cysteines in CstA$^{Rhod\text{-}TusA}$. We next sought to determine if Cys66 and Cys128 are capable of making close approach to another, at least transiently, to effect intramolecular persulfide transfer. To probe this, we used molecular oxygen, tetrathionate[51] (Figure 7) and Cu(II) salts[52] in an effort to form an intramolecular Cys66-Cys128 disulfide bond. Here, CstA$^{Rhod\text{-}TusA}$ (21.6 kDa) was left open to air, or incubated with either tetrathionate or $CuCl_2$ under anaerobic conditions, and the reaction products subjected to chromatography on a G75 column, with subsequent fractions electrophoresed on nonreducing SDS-PAGE gels.

We first chromatographed fully reduced and unmodified CstA on an analytical G75 column to provide a reference point for the cross-linking experiments (Figure 7A). CstA$^{Rhod\text{-}TusA}$ was found to be highly anisotropic given an apparent molecular weight of ∼32 kDa which is ∼1.5 times larger than expected for a spherical particle of 21.6 kDa. Treatment of wild-type, C66A, C128A CstA$^{Rhod\text{-}TusA}$ with molecular oxygen (Figure 7B) or 5 mol equiv of tetrathionate over Cys (Figure 7C) gives rise to both monomers and dimers, but to varying degrees. Both wild-type and C66A CstA$^{Rhod\text{-}TusA}$ give rise to a mixture of monomers and dimers, while C128A CstA$^{Rhod\text{-}TusA}$ is nearly exclusively monomeric under these conditions. This suggests that Cys128 from one protein molecule is at least transiently near Cys128′ from another resulting in the formation of cross-linked dimers. To confirm this, we electrophoresed the tetrathionate-oxidized products on a nonreducing gel (Figure 8). Remarkably, the monomer band is characterized by two differentially migrating species, one of which comigrates with authentic reduced CstA$^{Rhod\text{-}TusA}$ (labeled b) and the other of which runs with a significantly faster mobility, closer to the true molecular weight of CstA$^{Rhod\text{-}TusA}$ (labeled a) (Figure 8, compare middle and right panels). These two gel bands as well as the major dimer band (labeled c) were excised from the gel and subjected to in-gel tryptic digestion and analysis by mass spectrometry (Figures 8D and 9).

The faster migrating monomeric species uniquely contains an intramolecular Cys66-Cys128 cross-link as confirmed by high resolution mass spectrometry (Figure 9A) and tandem ESI-MS/MS (Figure 9C); this peptide is completely absent from the slower migrating species (band b) (Figure 8B). Band c contains a prominent Cys128-Cys128′ disulfide cross-link as expected (Figure 9B,D), but no detectable Cys66-Cys66′ or Cys66-Cys128 cross-link (Figure 8B). These data reveal that fully reduced CstA$^{Rhod\text{-}TusA}$ is structurally anisotropic and that

DOI: 10.1021/acs.biochem.5b00056
Biochemistry 2015, 54, 2385−2398

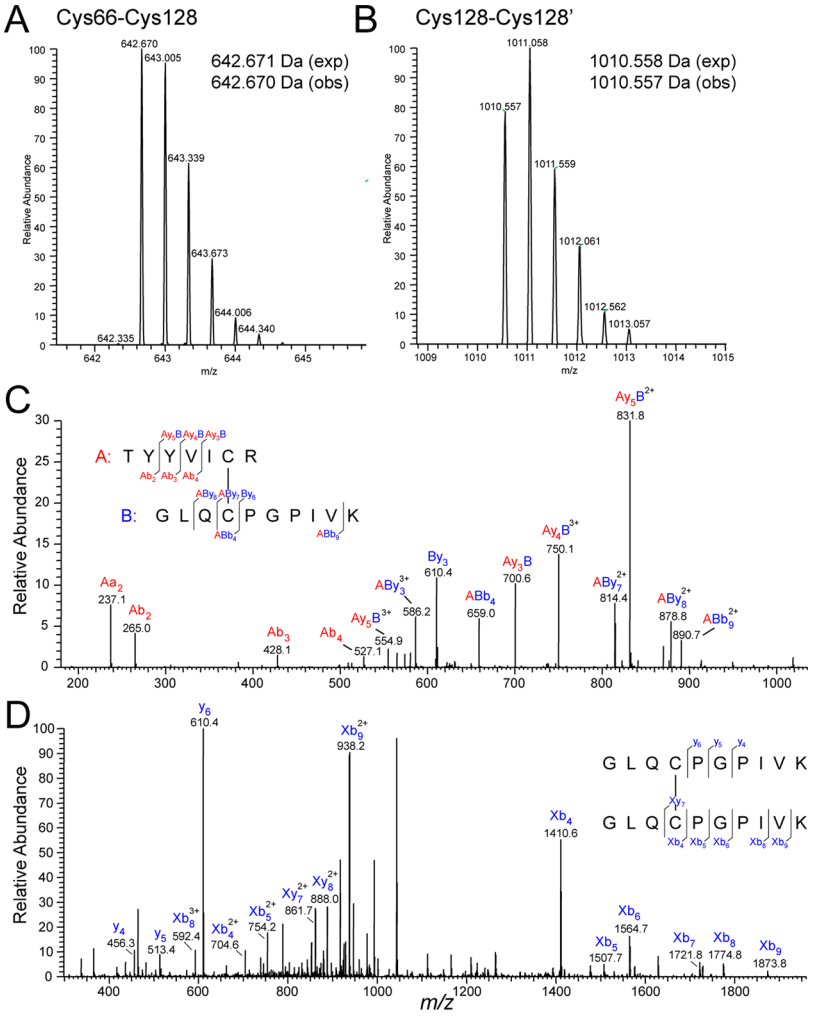

Figure 9. Analysis of disulfide cross-linked C66−C128 and C128−C128′ peptides by high-resolution tandem mass spectrometry recovered from monomer and dimer fractions of air-oxidized (24 h) wild-type CstA$^{Rhod\text{-}TusA}$. (A) High resolution masses determined for the tryptic peptides corresponding to an intramolecular disulfide bond between Cys66 and Cys128 (z = 3). (B) High resolution masses determined for the tryptic peptide corresponding to an intermolecular disulfide bond between Cys128 and Cys128′ (z = 3). (C) Tandem MS/MS fragmentation pattern of the peak shown in panel (A) and (D) Tandem MS/MS fragmentation pattern of the peak shown in panel (B). This analysis confirms the identity of the parent masses shown in panels (A) and (B). MALDI-MS data derived from gel bands a and c correspond to those spectra shown in Figure 5A, right.

intramolecular domain−domain cross-linking changes the shape of the molecule significantly, as evidenced by a change in mobility in a denaturing, nonreducing gel. However, intramolecular cross-linking between Cys66 and Cys128 is not clearly favored since intermolecular cross-linking between Cys128 residues on different monomers is competitive with intramolecular cross-linking. Nor does the reaction go to completion since significant reduced CstA$^{Rhod\text{-}TusA}$ is found in these reactions.

SAXS Analysis of CstA Domains. The experiments with reduced and monomeric CstA$^{Rhod\text{-}TusA}$ suggest an elongated molecule relative to CstA^{Rhod}. To learn more about global conformation of this two-domain molecule, we subjected both CstA$^{Rhod\text{-}TusA}$ and the isolated CstA^{Rhod} domain to small-angle X-ray scattering. Raw SAXS intensity scattering profiles are shown in Figure 10A (to q = 0.45 Å^{-1}), with pair distance distribution functions (PDDF) plots [P(r) vs r] shown in Figure 10B. Guinier plots (Figure 10A, inset) are indicative of monodispersity without aggregation, with the radius of gyration (R_g) significantly different between these two species, as expected (Table 1). The PDDF plots reveal that CstA$^{Rhod\text{-}TusA}$ is rod-like, with the range of pair distances extending to ∼110 Å, while the peak is asymmetrically positioned to far smaller distances relative to the maximum distance, D_{max}. In contrast, the isolated Rhod domain appears more globular, with an R_g value of 16−19 Å vs ∼30 Å for two domain CstA$^{Rhod\text{-}TusA}$ molecule (Table 1). For comparison, an R_g of ∼30 Å was recently measured for homotetrameric 48 kDa complex using identical methods.[53]

These features of the SAXS scattering curves and PDDF plots are recapitulated by the scattering envelopes calculated from these data (Figure 10C). The CstA$^{Rhod\text{-}TusA}$ is significantly elongated, with the scattering envelope of the CstA^{Rhod} superimposed using SUPCOMB into the "left" end of the two-domain molecule in the orientation shown. Although high resolution structures of the CstA$^{Rhod\text{-}TusA}$ or the isolated domains are not yet available, we position ribbon models of Rhod^a and TusA (pdb 3LVJ) domains of known structure into the scattering envelopes for reference (Figure 10C). We note that the orientation of the TusA domain is one of several that is consistent with the envelope. In any case, this model suggests that the two domains pack against one another "side-by-side" in the reduced state and must therefore adopt a more spherical

DOI: 10.1021/acs.biochem.5b00056
Biochemistry 2015, 54, 2385−2398

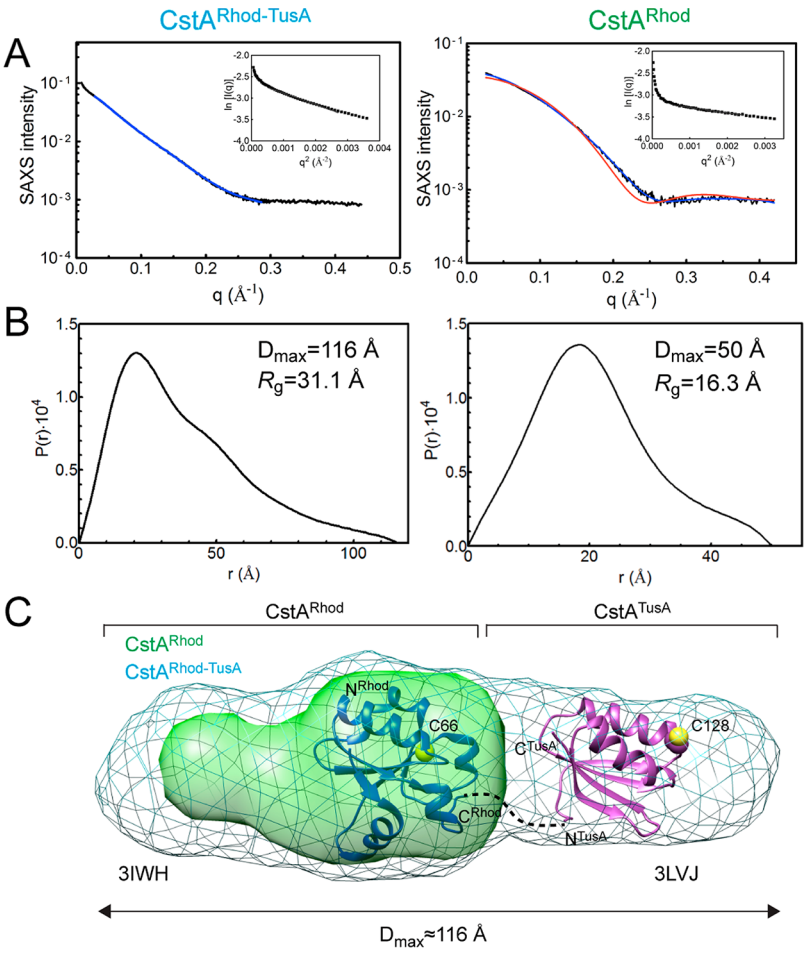

Figure 10. Analysis of reduced CstA$^{Rhod\text{-}TusA}$ and CstA^{Rhod} by small-angle X-ray scattering (SAXS). (A) Raw scattering intensity curves for CstA$^{Rhod\text{-}TusA}$ (left panel) and CstA^{Rhod} (right panel). Inset, Guinier approximations for each. The solid blue line for CstA^{Rhod} is calculated from the calculated scattering envelope, while the solid red line is calculated from the crystal structure of a model Rhod domain (pdb 3IWH) shown in panel C. (B) Real space pair distance distribution functions (PDDF) of CstA$^{Rhod\text{-}TusA}$ (left panel) and CstA^{Rhod} (right panel) derived from the scattering curves (panel A). (C) Scattering envelopes of CstA$^{Rhod\text{-}TusA}$ and CstA^{Rhod} using DAMMIF and DAMAVER as described in Materials and Methods, with CstA^{Rhod} envelope superimposed on CstA$^{Rhod\text{-}TusA}$ using SUPCOMB.[45] These data reveal that the CstA^{Rhod} domain (shaded green) superimposes well on the "left"-half of the full envelope calculated for CstA$^{Rhod\text{-}TusA}$ (shaded light blue), which agrees well with the experimental raw scattering data (panel A, right) and an envelope calculated for the known Rhod structure (*S. aureus* COL SACOL1807 in ribbon; pdb 3IWH). The orientation of the TusA domain is one of several that is consistent with the envelope and with structurally known TusA-like domains (pdb 3LVJ ribbon shown). Cα atoms of what would correspond to Cys66 and Cys128 are represented as yellow spheres.

structure in order to form an C66−C128 disulfide bond as a mimic of a persulfide transfer intermediate (Figure 8).

DISCUSSION

This work summarizes biochemical and structural insights into the multidomain sulfurtransferase *S. aureus* CstA through characterization of the N-terminal Rhod and two domain CstA$^{Rhod\text{-}TusA}$ proteins (see Figure 1). We establish here and in other work[12] that the *cst* operon is induced by hydrogen sulfide, and that CstA is a *bona fide* sulfurtransferase required to protect *S. aureus* against hydrogen sulfide toxicity. However, the function of the C-terminal TusD domain in CstA remains unclear as does the mechanism by which CstA functions in hydrogen sulfide detoxification in the cell. The rod-like structure of CstA$^{Rhod\text{-}TusA}$ might allow for rapid binding of an activated cysteine desulfurase, e.g., a NifS or SufS, hypothesized to be associated with 4-thiouridine and/or thiamin biosynthesis and Fe−S protein biogenesis, respectively,[17,54] to the TusA domain. In 2-thiouridine biosynthesis in *E. coli*, for example, TusA is known to physically interact with the IscS dimer[17] and this interaction stimulates persulfide transfer to the Cys active site of TusA. TusA then passes the persulfide to TusD in the TusBCD complex, which is then transferred to TusE and ultimately to MnmA which catalyzes sulfur insertion to make 2-thiouridine in the Wobble position (U34) in tRNA.[54] Thus, the TusA domain of CstA may be the entry point for persulfide transfer from SufS/IscS to the C-terminal TusD domain (see Figure 1).

We show here that persulfurated SufS can indeed function as a persulfide donor to CstA with high efficiency (Figure 6); however, this reaction appears dependent on C66 in the Rhod domain. Previous studies in *Azotobacter vinelandii* provide evidence for an intermolecular disulfide bond formed by the active site cysteines of the rhodanese RhdA and the cysteine desulfurase IscS at limiting [cysteine], thus mimicking a persulfide transfer intermediate.[38] One exciting possibility is that SufS and CstA form a complex that alters the relative orientations of the Rhod and TusA domains, enhancing sequential persulfide shuttling to the downstream acceptor C128. More generally, coimmunoprecipitation experiments with affinity-tagged CstA would allow identification of those proteins that physically interact

DOI: 10.1021/acs.biochem.5b00056
Biochemistry 2015, 54, 2385−2398

with various domains of CstA and function as downstream targets under conditions of sulfide toxicity (see Figure 1). Potential targets include the dithiol thioredoxins,[55] the putative persulfide dioxygenase CstB or proteins involved in Fe−S or molybdopterin cofactor maturation[56] that might serve to detoxify or assimilate sulfur under these conditions of high sulfur mobilization.

The double rhodanese homology domain protein RhdA from *Azotobacter vinelandii*, which contains a single Cys in the C-terminal Rhod domain, has been shown to contribute to cellular redox balance. In the presence of oxidizing conditions capable of generating glutathionyl radical GS•, RhdA can catalyze the regeneration of reduced glutathione (GSH) via a formation of a mixed disulfide with GSH, which is released as GSSG. RhdA possesses a micromolar K_m for GSH, far lower than that measured for TS; it is not yet known if tight binding of LMW thiols is a general property of all Rhod domains. In this context, it is worth pointing out that a major consequence of hydrogen sulfide stress is hypothesized to be the persulfuration and poly-*S*-sulfhydration of protein and LMW thiols via direct attack of HS^- on a LMW disulfide.[12] It therefore seems plausible that the N-terminal domain of CstA may have evolved to bind glutathione persulfide, GSSH, or some other low molecular weight persulfide and perform nucleophilic attack on the terminal sulfur to regenerate the reduced thiol, e.g., GSH, and an CstA-bound persulfide. The regulator of the *cst* operon, CstR, performs exactly this chemistry.[12]

Finally, our low resolution model of a highly anisotropic $CstA^{Rhod\text{-}TusA}$ (Figure 10C) may represent a conformation that is intrinsically weakly active in persulfide transfer with inorganic sulfur donors (Figures 4 and 5) due specifically to the lack of the C-terminal TusD domain. This seems unlikely due to the apparent modular nature of these proteins as evidenced by inspection of the genome organization of *cstA*-like genes in other organisms. However, other homooligomeric TusD- or DsrE-like proteins, e.g., *E. coli* YchN,[19] are known to be trimeric; this, in turn, suggests the possibility that the TusD domain mediates oligomer (trimer) formation in CstA, which would then stabilize what must be weak interactions between the TusA domains observed here as Cys128-Cys128′ cross-links (Figures 8 and 9). Formation of a higher order structure may allosterically stabilize a "closed," more globular Rhod-TusA structure more suitable for persulfide transfer that is mimicked by the Cys66-Cys128 cross-linked structure trapped here (Figure 8) and in reactions using SufS as a sulfane sulfur donor (Figure 6). Alternatively, persulfuration drives a change in global conformation and/or dynamics of $CstA^{Rhod\text{-}TusA}$ in a way that stimulates efficient persulfide transfer. We point out that it is not firmly established that both Cys66 and Cys128 can be persulfurated on the same $CstA^{Rhod\text{-}TusA}$ molecule since the analysis presented here is focused on identification *S*-sulfhydrated tryptic peptides; however, given the generally low yield of Cys128 persulfide, this seems likely to be the case. NMR structural studies designed to map changes in conformation and dynamics in both $CstA^{Rhod\text{-}TusA}$ and intact CstA upon persulfuration, coupled with functional studies to identify downstream proteins that accept CstA-derived persulfides (see Figure 1), will be required to shed additional light on the role of CstA in sulfide homeostasis and detoxification in this important human pathogen.

■ ASSOCIATED CONTENT

Supporting Information

Tables S1−S3 and Figures S1−S3. This material is available free of charge via the Internet at http://pubs.acs.org.

■ AUTHOR INFORMATION

Corresponding Author

*Tel: 812-856-3178. Fax: 812-856-5710. E-mail: giedroc@indiana.edu.

Present Address

[#]Department of Chemistry, Salve Regina University, 100 Ochre Point Avenue, Newport, RI 02840, USA.

Funding

The authors gratefully acknowledge financial support of the National Institutes of Health (R01 GM097225) to D.P.G.

Notes

The authors declare no competing financial interest.

■ ABBREVIATIONS

Cst, CsoR-like sulfurtransferase; Dsr, dissimilatory sulfite reductase; Rhod, rhodanese; SAXS, small-angle X-ray scattering; TS, thiosulfate; TST, thiosulfate sulfurtransferase; Tus, tRNA 2-thiouridine synthesizing protein

■ ADDITIONAL NOTE

[a]Unpublished structure deposition under PDB accession code 3IWH.

■ REFERENCES

(1) Moen, A. E., Storla, D. G., Bukholm, G. Distribution of methicillin-resistant *Staphylococcus aureus* in a low-prevalence area. *FEMS Immunol. Med. Microbiol. 58*, 374−380.

(2) Shatalin, K., Shatalina, E., Mironov, A., and Nudler, E. (2011) H_2S: a universal defense against antibiotics in bacteria. *Science 334*, 986−990.

(3) Schelle, M. W., and Bertozzi, C. R. (2006) Sulfate metabolism in mycobacteria. *ChemBiochem 7*, 1516−1524.

(4) Bhave, D. P., Muse, W. B., 3rd, and Carroll, K. S. (2007) Drug targets in mycobacterial sulfur metabolism. *Infect. Disord. Drug Targets 7*, 140−158.

(5) Burns, K. E., Baumgart, S., Dorrestein, P. C., Zhai, H., McLafferty, F. W., and Begley, T. P. (2005) Reconstitution of a new cysteine biosynthetic pathway in *Mycobacterium tuberculosis*. *J. Am. Chem. Soc. 127*, 11602−11603.

(6) Hong, J. A., Bhave, D. P., and Carroll, K. S. (2009) Identification of critical ligand binding determinants in *Mycobacterium tuberculosis* adenosine-5′-phosphosulfate reductase. *J. Med. Chem. 52*, 5485−5495.

(7) Senaratne, R. H., Mougous, J. D., Reader, J. R., Williams, S. J., Zhang, T., Bertozzi, C. R., and Riley, L. W. (2007) Vaccine efficacy of an attenuated but persistent *Mycobacterium tuberculosis cysH* mutant. *J. Med. Microbiol. 56*, 454−458.

(8) Ma, Z., Cowart, D. M., Scott, R. A., and Giedroc, D. P. (2009) Molecular insights into the metal selectivity of the copper(I)-sensing repressor CsoR from *Bacillus subtilis*. *Biochemistry 48*, 3325−3334.

(9) Liu, T., Ramesh, A., Ma, Z., Ward, S. K., Zhang, L., George, G. N., Talaat, A. M., Sacchettini, J. C., and Giedroc, D. P. (2007) CsoR is a novel *Mycobacterium tuberculosis* copper-sensing transcriptional regulator. *Nat. Chem. Biol. 3*, 60−68.

(10) Grossoehme, N., Kehl-Fie, T. E., Ma, Z., Adams, K. W., Cowart, D. M., Scott, R. A., Skaar, E. P., and Giedroc, D. P. (2011) Control of copper resistance and inorganic sulfur metabolism by paralogous regulators in *Staphylococcus aureus*. *J. Biol. Chem. 286*, 13522−13531.

(11) Luebke, J. L., Arnold, R. J., and Giedroc, D. P. (2013) Selenite and tellurite form mixed seleno- and tellurotrisulfides with CstR from *Staphylococcus aureus*. *Metallomics 5*, 335−342.

(12) Luebke, J. L., Shen, J., Bruce, K. E., Kehl-Fie, T. E., Peng, H., Skaar, E. P., and Giedroc, D. P. (2014) The CsoR-like sulfurtransferase repressor (CstR) is a persulfide sensor in *Staphylococcus aureus*. *Mol. Microbiol. 94*, 1343−1360.

DOI: 10.1021/acs.biochem.5b00056
Biochemistry 2015, 54, 2385−2398

(13) Cipollone, R., Ascenzi, P., and Visca, P. (2007) Common themes and variations in the rhodanese superfamily. *IUBMB Life 59*, 51−59.
(14) Mueller, E. G. (2006) Trafficking in persulfides: delivering sulfur in biosynthetic pathways. *Nat. Chem. Biol. 2*, 185−194.
(15) Lill, R., Diekert, K., Kaut, A., Lange, H., Pelzer, W., Prohl, C., and Kispal, G. (1999) The essential role of mitochondria in the biogenesis of cellular iron-sulfur proteins. *Biol. Chem. 380*, 1157−1166.
(16) Kabil, O., and Banerjee, R. (2010) Redox biochemistry of hydrogen sulfide. *J. Biol. Chem. 285*, 21903−21907.
(17) Shi, R., Proteau, A., Villarroya, M., Moukadiri, I., Zhang, L., Trempe, J. F., Matte, A., Armengod, M. E., and Cygler, M. (2010) Structural basis for Fe-S cluster assembly and tRNA thiolation mediated by IscS protein-protein interactions. *PLoS Biol. 8*, e1000354.
(18) Numata, T., Fukai, S., Ikeuchi, Y., Suzuki, T., and Nureki, O. (2006) Structural basis for sulfur relay to RNA mediated by heterohexameric TusBCD complex. *Structure 14*, 357−366.
(19) Dahl, C., Schulte, A., Stockdreher, Y., Hong, C., Grimm, F., Sander, J., Kim, R., Kim, S. H., and Shin, D. H. (2008) Structural and molecular genetic insight into a widespread sulfur oxidation pathway. *J. Mol. Biol. 384*, 1287−1300.
(20) Li, H., Yang, F., Kang, X., Xia, B., and Jin, C. (2008) Solution structures and backbone dynamics of *Escherichia coli* rhodanese PspE in its sulfur-free and persulfide-intermediate forms: implications for the catalytic mechanism of rhodanese. *Biochemistry 47*, 4377−4385.
(21) Bordo, D., Deriu, D., Colnaghi, R., Carpen, A., Pagani, S., and Bolognesi, M. (2000) The crystal structure of a sulfurtransferase from *Azotobacter vinelandii* highlights the evolutionary relationship between the rhodanese and phosphatase enzyme families. *J. Mol. Biol. 298*, 691−704.
(22) Ploegman, J. H., Drent, G., Kalk, K. H., Hol, W. G., Heinrikson, R. L., Keim, P., Weng, L., and Russell, J. (1978) The covalent and tertiary structure of bovine liver rhodanese. *Nature 273*, 124−129.
(23) Hanzelmann, P., Dahl, J. U., Kuper, J., Urban, A., Muller-Theissen, U., Leimkuhler, S., and Schindelin, H. (2009) Crystal structure of YnjE from *Escherichia coli*, a sulfurtransferase with three rhodanese domains. *Protein Sci. 18*, 2480−2491.
(24) Dahl, J. U., Urban, A., Bolte, A., Sriyabhaya, P., Donahue, J. L., Nimtz, M., Larson, T. J., and Leimkuhler, S. (2011) The identification of a novel protein involved in molybdenum cofactor biosynthesis in *Escherichia coli*. *J. Biol. Chem. 286*, 35801−35812.
(25) Palenchar, P. M., Buck, C. J., Cheng, H., Larson, T. J., and Mueller, E. G. (2000) Evidence that ThiI, an enzyme shared between thiamin and 4-thiouridine biosynthesis, may be a sulfurtransferase that proceeds through a persulfide intermediate. *J. Biol. Chem. 275*, 8283−8286.
(26) Matthies, A., Nimtz, M., and Leimkuhler, S. (2005) Molybdenum cofactor biosynthesis in humans: identification of a persulfide group in the rhodanese-like domain of MOCS3 by mass spectrometry. *Biochemistry 44*, 7912−7920.
(27) Wallen, J. R., Mallett, T. C., Boles, W., Parsonage, D., Furdui, C. M., Karplus, P. A., and Claiborne, A. (2009) Crystal structure and catalytic properties of *Bacillus anthracis* CoADR-RHD: implications for flavin-linked sulfur trafficking. *Biochemistry 48*, 9650−9667.
(28) Tombline, G., Schwingel, J. M., Lapek, J. D., Jr., Friedman, A. E., Darrah, T., Maguire, M., Van Alst, N. E., Filiatrault, M. J., and Iglewski, B. H. (2013) Pseudomonas aeruginosa PA1006 is a persulfide-modified protein that is critical for molybdenum homeostasis. *PloS One 8*, e55593.
(29) Filiatrault, M. J., Tombline, G., Wagner, V. E., Van Alst, N., Rumbaugh, K., Sokol, P., Schwingel, J., and Iglewski, B. H. (2013) *Pseudomonas aeruginosa* PA1006, which plays a role in molybdenum homeostasis, is required for nitrate utilization, biofilm formation, and virulence. *PloS One 8*, e55594.
(30) Chng, S. S., Dutton, R. J., Denoncin, K., Vertommen, D., Collet, J. F., Kadokura, H., and Beckwith, J. (2012) Overexpression of the rhodanese PspE, a single cysteine-containing protein, restores disulphide bond formation to an *Escherichia coli* strain lacking DsbA. *Mol. Microbiol. 85*, 996−1006.
(31) Cheng, H., Donahue, J. L., Battle, S. E., Ray, W. K., and Larson, T. J. (2008) Biochemical and Genetic Characterization of PspE and GlpE, Two Single-domain Sulfurtransferases of *Escherichia coli*. *Open Microbiol J. 2*, 18−28.
(32) Wallrodt, I., Jelsbak, L., Thorndahl, L., Thomsen, L. E., Lemire, S., and Olsen, J. E. (2013) The putative thiosulfate sulfurtransferases PspE and GlpE contribute to virulence of *Salmonella Typhimurium* in the mouse model of systemic disease. *PloS One 8*, e70829.
(33) Sheffield, P., Garrard, S., and Derewenda, Z. (1999) Overcoming expression and purification problems of RhoGDI using a family of "parallel" expression vectors. *Protein Expr. Purif. 15*, 34−39.
(34) Bubeck Wardenburg, J., Williams, W. A., and Missiakas, D. (2006) Host defenses against *Staphylococcus aureus* infection require recognition of bacterial lipoproteins. *Proc. Natl. Acad. Sci. U. S. A. 103*, 13831−13836.
(35) Toledo-Arana, A., Merino, N., Vergara-Irigaray, M., Debarbouille, M., Penades, J. R., and Lasa, I. (2005) *Staphylococcus aureus* develops an alternative, *ica*-independent biofilm in the absence of the *arlRS* two-component system. *J. Bacteriol. 187*, 5318−5329.
(36) Hussain, M., Hastings, J. G. M., and White, P. J. (1991) A chemically defined medium for slime production by coagulase-negative staphylococci. *J. Med. Microbiol. 34*, 143−147.
(37) Yadav, P. K., Yamada, K., Chiku, T., Koutmos, M., and Banerjee, R. (2013) Structure and kinetic analysis of H_2S production by human mercaptopyruvate sulfurtransferase. *J. Biol. Chem. 288*, 20002−20013.
(38) Giuliani, M. C., Tron, P., Leroy, G., Aubert, C., Tauc, P., and Giudici-Orticoni, M. T. (2007) A new sulfurtransferase from the hyperthermophilic bacterium *Aquifex aeolicus*. Being single is not so simple when temperature gets high. *FEBS J. 274*, 4572−4587.
(39) Forlani, F., Cereda, A., Freuer, A., Nimtz, M., Leimkuhler, S., and Pagani, S. (2005) The cysteine-desulfurase IscS promotes the production of the rhodanese RhdA in the persulfurated form. *FEBS Lett. 579*, 6786−6790.
(40) Senko, M., Beu, S., and McLaffertycor, F. (1995) Determination of monoisotopic masses and ion populations for large biomolecules from resolved isotopic distributions. *J. Am. Soc. Mass Spectrom. 6*, 229−233.
(41) Ma, Z., Cowart, D. M., Ward, B. P., Arnold, R. J., DiMarchi, R. D., Zhang, L., George, G. N., Scott, R. A., and Giedroc, D. P. (2009) Unnatural amino acid substitution as a probe of the allosteric coupling pathway in a mycobacterial Cu(I) sensor. *J. Am. Chem. Soc. 131*, 18044−18045.
(42) Konarev, P. V., Volkov, V. V., Sokolova, A. V., Koch, M. H. J., and Svergun, D. I. (2003) PRIMUS: a Windows PC-based system for small-angle scattering data analysis. *J. Appl. Crystallogr. 36*, 1277−1282.
(43) Svergun, D. I. (1992) Determination of the regularization parameter in indirect-transform methods using perceptual criteria. *J. Appl. Crystallogr. 25*, 495−503.
(44) Hura, G. L., Menon, A. L., Hammel, M., Rambo, R. P., Poole, F. L., 2nd, Tsutakawa, S. E., Jenney, F. E., Jr., Classen, S., Frankel, K. A., Hopkins, R. C., Yang, S. J., Scott, J. W., Dillard, B. D., Adams, M. W., and Tainer, J. A. (2009) Robust, high-throughput solution structural analyses by small angle X-ray scattering (SAXS). *Nat. Methods 6*, 606−612.
(45) Kozin, M., and Svergun, D. I. (2001) Automated matching of high- and low-resolution structural models. *J. Appl. Crystallogr. 34*, 39−41.
(46) Schneidman-Duhovny, D., Hammel, M., and Sali, A. (2010) FoXS: a web server for rapid computation and fitting of SAXS profiles. *Nucleic Acids Res. 38*, W540−544.
(47) Schneidman-Duhovny, D., Hammel, M., Tainer, J. A., and Sali, A. (2013) Accurate SAXS profile computation and its assessment by contrast variation experiments. *Biophys. J. 105*, 962−974.
(48) Remelli, W., Guerrieri, N., Klodmann, J., Papenbrock, J., Pagani, S., and Forlani, F. (2012) Involvement of the *Azotobacter vinelandii* rhodanese-like protein RhdA in the glutathione regeneration pathway. *PloS One 7*, e45193.

DOI: 10.1021/acs.biochem.5b00056
Biochemistry 2015, 54, 2385−2398

(49) Greiner, R., Palinkas, Z., Basell, K., Becher, D., Antelmann, H., Nagy, P., and Dick, T. P. (2013) Polysulfides link H_2S to protein thiol oxidation. *Antioxid. Redox Signal. 19*, 1749−1765.
(50) Pan, J., and Carroll, K. S. (2013) Persulfide reactivity in the detection of protein *S*-sulfhydration. *ACS Chem. Biol. 8*, 1110−1116.
(51) Prasad, A. R., and Horowitz, P. M. (1987) Chemical modification of bovine liver rhodanese with tetrathionate: differential effects on the sulfur-free and sulfur-containing catalytic intermediates. *Biochim. Biophys. Acta 911*, 102−108.
(52) Hao, Z., Lou, H., Zhu, R., Zhu, J., Zhang, D., Zhao, B. S., Zeng, S., Chen, X., Chan, J., He, C., and Chen, P. R. (2014) The multiple antibiotic resistance regulator MarR is a copper sensor in Escherichia coli. *Nat. Chem. Biol. 10*, 21−28.
(53) Chang, F.-M., Coyne, H. J., III, Ramirez, C. A. C., Fleischmann, P. V., Fang, X., Ma, Z., Ma, D., Helmann, J. D., García-de los Santos, A., Wang, Y.-X., Dann, C. E., III, and Giedroc, D. P. (2014) Cu(I)-mediated allosteric switching in a copper-sensing operon repressor (CsoR). *J. Biol. Chem. 289*, 19204−19217.
(54) Ikeuchi, Y., Shigi, N., Kato, J., Nishimura, A., and Suzuki, T. (2006) Mechanistic insights into sulfur relay by multiple sulfur mediators involved in thiouridine biosynthesis at tRNA wobble positions. *Mol. Cell 21*, 97−108.
(55) Ray, W. K., Zeng, G., Potters, M. B., Mansuri, A. M., and Larson, T. J. (2000) Characterization of a 12-kilodalton rhodanese encoded by *glpE* of *Escherichia coli* and its interaction with thioredoxin. *J. Bacteriol. 182*, 2277−2284.
(56) Cereda, A., Forlani, F., Iametti, S., Bernhardt, R., Ferranti, P., Picariello, G., Pagani, S., and Bonomi, F. (2003) Molecular recognition between *Azotobacter vinelandii* rhodanese and a sulfur acceptor protein. *Biol. Chem. 384*, 1473−1481.

DOI: 10.1021/acs.biochem.5b00056
Biochemistry 2015, 54, 2385−2398